
2 Fundamentals

In this chapter the theoretical framework of this work will be outlined. In the first part the structure and some important properties of the layered dichalcogenides will be described. In the second part the intercalation reaction will be introduced and reviewed with particular emphasis to this class of materials. Only some essential aspects will be given mainly based on the reviews cited in each section.

2.1 Transition metal dichalcogenides

The class of compounds known as transition metal dichalcogenides (TMDCs) consists of about 60 compounds of the general formula MX_2 , where X is a chalcogen (S, Se, Te), and M is Re, Pt, Sn, Pb, or a transition metal of the groups IVb, Vb, VIb. Some comprehensive reviews describe their structural, electronic, and optical properties [14, 18, 29].

2.1.1 Crystal structure

Most TMDCs form hexagonal layered structures. The repeating 2-D unit is a slab formed by a plane of M atoms, in between two planes of chalcogen X. Interactions between atoms in a slab are mainly covalent, while only saturated orbitals of the chalcogens are exposed to the exterior. Slab-to-slab interactions are 1 to 2 orders of magnitude weaker than within a slab. These weak interactions are generally referred to as of the van der Waals type, even though a covalent coupling is also possible [33]. Therefore cleavage along the interlayer gap (van der Waals gap) is easy, and in ideal cases, perfect dangling bond-free surfaces can be obtained by peeling off a scotch tape attached to a crystal. The hexagonally close packed surfaces of the cleavage plane are for this reason called van der Waals surfaces. Since the strength of interactions is remarkably larger within the slabs, the chemical and physical properties are anisotropic and usually considered as nearly two-dimensional.

The metal atom is always coordinated by six chalcogenides. Two geometries are possible: trigonal prismatic and trigonal antiprismatic (commonly referred to as octahedral, although distorted). The preferred coordination is determined by the bond ionicity as given by the electronegativity difference between metal and chalcogen. Octahedral coordination is preferred in more ionic compounds, since it maximizes the distance between negatively charged chalcogens. On the other hand the overlap between metal and chalcogen wave functions is optimized in a trigonal prismatic coordination [33], which is typically found for more covalent compounds.

Due to the weak interlayer interactions, several different slab-stacking sequences (crystal polytypes) are found. The free energy of formation of the different polytypes is similar and the

transition requires a low activation energy. For this reason TMDCs are also used as solid state lubricants [10, 11, 13, 38, 39].

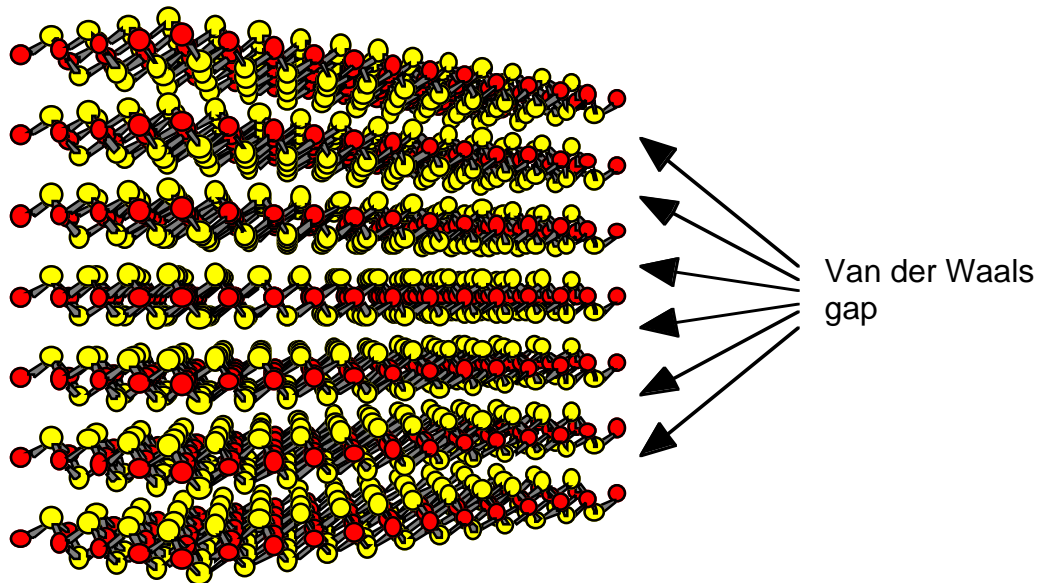


Fig. 2.1 The sandwich-like structure of layered chalcogenides

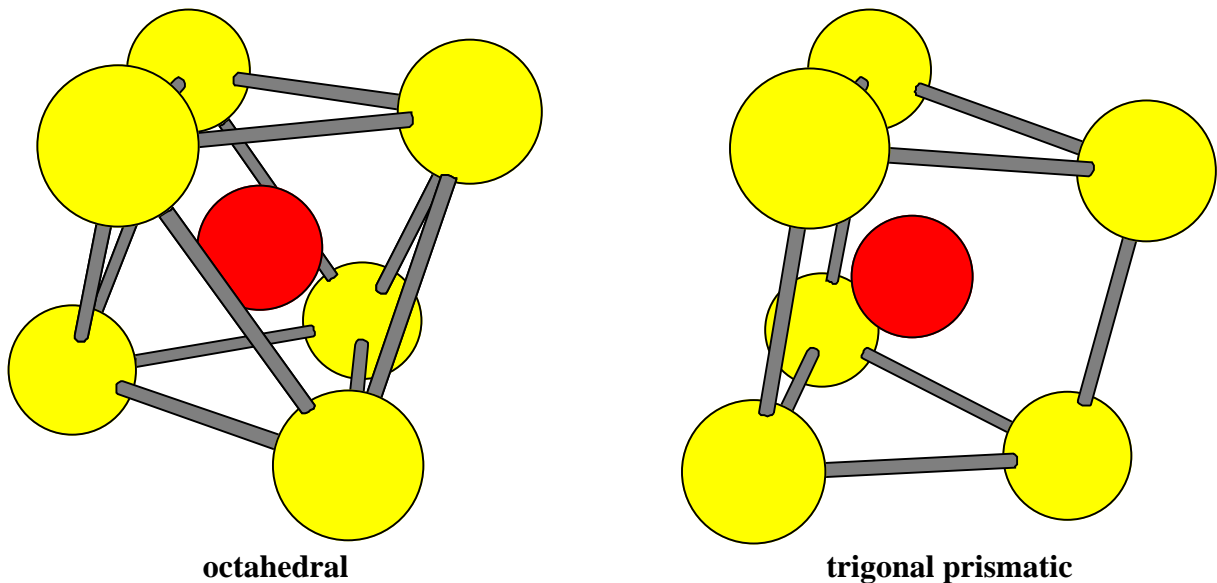


Fig. 2.2 The two coordination polyhedrons for the transition metal in layered chalcogenides. The drawn lines stress the geometry and do not refer to chemical interactions

The unit cell is defined with the c axis perpendicular to the layers, and the \mathbf{a} and \mathbf{b} axes along the minimal chalcogen-chalcogen distance. In a close-packed stacking the hexagonal lattice planes can occupy one of three equivalent positions. If atoms of a plane occupy the position A (i.e. at the origin of the \mathbf{a} - \mathbf{b} two-dimensional unit cell, as in Fig. 2.3a), atoms of the next planes can occupy either position B or C. In dependence of the contained species, each atomic plane can be indicated as A, B, C for the chalcogen, a, b, c for the transition metal, [a], [b], [c] for possible guest species. According to this notation the trigonal prismatic coordination is indicated with AbA, while

the octahedral is AbC. Many possible layer stackings exist if we consider that alternated trigonal prismatic and octahedral structures are also known.

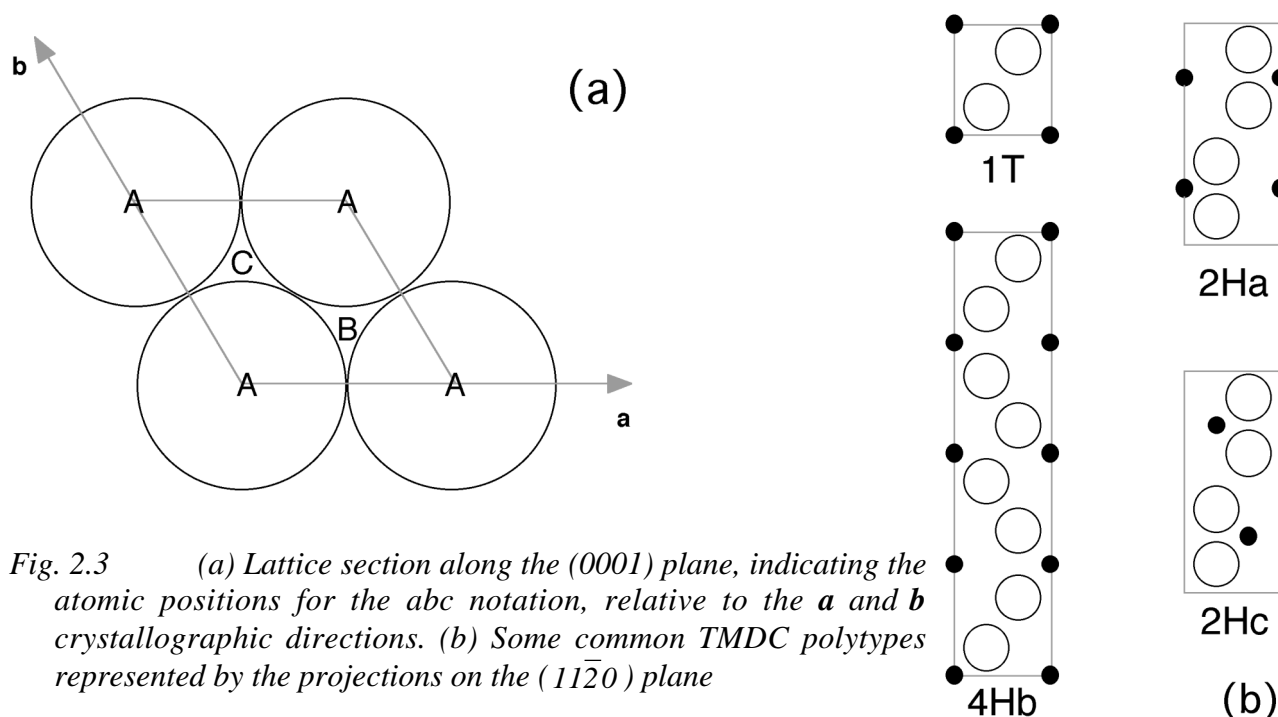


Fig. 2.3 (a) Lattice section along the (0001) plane, indicating the atomic positions for the abc notation, relative to the *a* and *b* crystallographic directions. (b) Some common TMDC polytypes represented by the projections on the $(11\bar{2}0)$ plane

phase	space group	metal coordination	plane sequence
1T	$P\bar{3}m1$	octahedral	AbC
2Ha	$P6_3/mmc$	trigonal prismatic	BcB AcA
2Hb	$P6m2$	trigonal prismatic	BcB AbA
2Hc	$P6_3/mmc$	trigonal prismatic	BaB AbA
3R	$R3m$	trigonal prismatic	BcB CaC AbA
4Ha	$P\bar{6}m2$	trigonal prismatic	BcB AcA BcB CaC
4Hb	$P6_3/mmc$	mixed	BcB CaB CaC BaC
4Hc	$P6_3mc$	trigonal prismatic	BcB AcA BaB CaC
4HdI	$P3m1$	mixed	BcA BcB CaB AcA
4HdII	$P6m2$	mixed	AcA BcA BaB AcB
6R	$R3m$	mixed	BcB CaB CaC AbC AbA BcA

Tab. 2.1 Most common polytypes found in TMDCs

A rationalized nomenclature uses a number and a letter to identify the polytypes. The number indicates how many layers are included in the unit cell, and the letter can be T (trigonal), H (hexagonal) or R (rhomboedrical). Small letters can distinguish among different polytypes. The most common structures have the lowest numbers of layers in the unit cell, so that the typical form for the octahedral coordination is 1T, and 2H for the trigonal prismatic. The different polytypes are typically represented by their section through the $(11\bar{2}0)$ plane (Fig. 2.3b).

Due to the hexagonal chalcogen packing and the compact interlayer stacking only octahedral and tetrahedral interstitial sites are present in the van der Waals gap. Regardless of the symmetry there are one octahedral and two tetrahedral sites for each transition metal center.

2.1.2 Electronic structure

The optical properties of TMDCs were first explained in terms of their electronic bands by Wilson and Joffe [14] in a model, which has been improved by theoretical calculations and experimental data, but so far has not been contradicted [16]. A scheme is reported in Fig. 2.4. Although the bond is known to be only 10-30% ionic [33], the compound is assumed as totally ionic in this model. The transition metal has $s^2p^6d^x$ electron configuration, where $x=0, 1$ or 2 , depending on whether the metal belongs to the group IVb, Vb or VIb. The s and p valence orbitals from the metal overlap with corresponding chalcogen p orbitals, which have a larger ionization potential. The resulting bonding and antibonding bands separate by 5-10 eV. Due to the different energy of the atomic orbitals the bonding bands have chalcogen and the antibonding metal character. The metal d states instead are mostly unperturbed by the interaction, and typically remain located in the gap between bonding and antibonding states. Due to the two-dimensional structure of these materials, the electronic structure is much less affected by the layer stacking than by the symmetry of the metal coordination. The octahedral crystal field splits the d levels in two bands with e_g and t_{2g} symmetry, respectively. The e_g band corresponds to d_{xz} and d_{yz} orbitals which interact more with the chalcogen, and are found at higher energy. The trigonal distortion from the regular octahedral coordination can be measured as deviation from the ideal value of 0.816 from the ratio between layer thickness and the lattice constant a . But more easily available is the ratio c/a , which is 1.633 for perfect octahedral coordination. Calculations and photoemission measurements show that the d_{z^2} band position is mainly affected by the octahedral distortion; if the coordination is prismatic its position is even distinct from the rest of the d bands. The band occupancy above the filled chalcogen p valence band determines whether the TMDC is a metal, semimetal or semiconductor. The d_{z^2} band is half-filled in the case of compounds of group Vb metals, and they exhibit metallic conductivity. This band is completely filled in the case of the group VIb, and the chalcogenides are semiconductors. The nature of group IVb compounds depends on the distance between the empty d_{z^2} band and the p bands below. As an example $TiSe_2$ is a semimetal, while for TiS_2 a precise evaluation from calculations or measurements is not straightforward, and it is still debated whether it is a semimetal or a semiconductor [40].

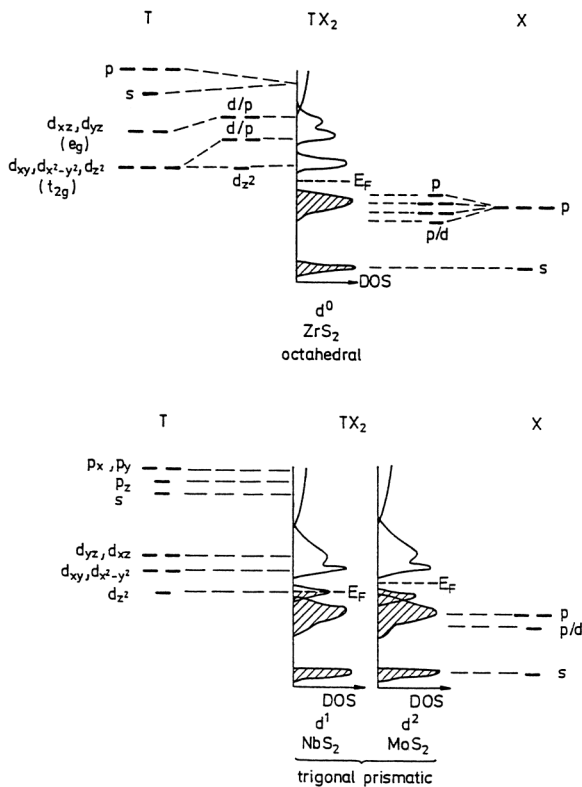


Fig. 2.4 Schematic diagrams of the density of states for TMDCs of groups IVb-Vb-VIb after the Wilson and Yoffe model. From ref. [32]

The Brillouin zone for the hexagonal crystal structure is reported in Fig. 2.5. Several electronic structures have been published in the last 30 years (see e.g. [40-46]). With the exception of the relative energies of the bands and the position of the Fermi level, the form of the bands found with all recent self-consistent calculation are in good agreement to each other. Many similarities are found among structures of different compounds having the same transition metal coordination. As an example, the structure of 1T-TiS₂ is reported in Fig. 2.5b. The 6 bands below E_F have mainly S 3p character, while the next 5 consist essentially of Ti 3d states. Of these 5, the lower group of 3 corresponds to the crystal-field split t_{2g} and the next 2 to e_g bands. The two S 3p bands with stronger dispersion in ΓA are mainly p_z orbitals, and the dispersion is essentially due to the intra-layer interaction. For TiS₂ most recent calculations report an overlap between the top S 3p bands in Γ and the minimum of the Ti 3d band in L. Photoemission measurements tend to indicate rather a small gap of 0.2 eV [40, 47]. Fang *et al.* attempted to explain this disagreement by showing that for single slabs, without the inter-layer interaction, a band gap can be predicted. In a similar way, surface sensitive measurements would overestimate the contribution of the semiconducting top layer [40].

Many metallic TMDCs exhibit at low temperature the phenomenon of Peierl's distortions, or charge density waves (CDWs), a stabilization of the conduction electrons by a periodic lattice distortion which results in an uneven spatial distribution of free charge carriers [1, 48, 49]. In presence of CDWs, the conductivity is reduced. The energetic advantage of distortion to stabilize

valence electrons is particularly large for TMDCs of the group Vb. To stabilize the only d_{z^2} electron 1T-TaS₂ and 1T-TaSe₂ show CDWs still at room temperature. In this case CDW effects are so pronounced that practically the existence of Ta³⁺, Ta⁴⁺, Ta⁵⁺ can be considered. Consequently, different equivalent Ta positions will result, as evidenced by the chemical shift of the Ta core level signal in SXPS experiments [50-53]. Different phases are formed in dependence of the temperature, and their period is typically not commensurate with the crystal lattice. Nevertheless, when the interaction is particularly strong a pinning can take place so that the CDW and the crystal period are related, and the CDW phase is said to be commensurate.

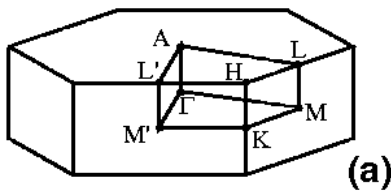
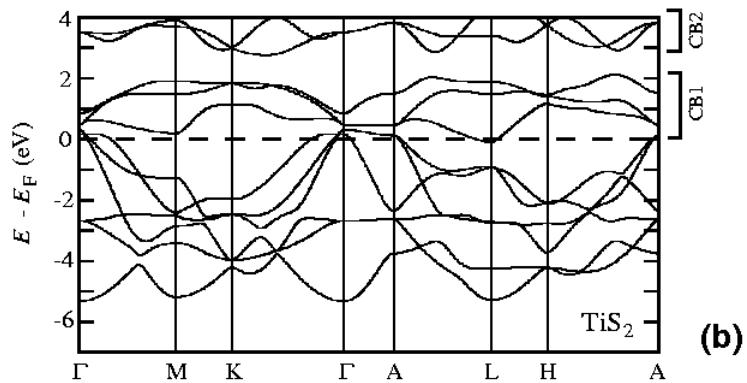


Fig. 2.5 (a) First Brillouin zone of an hexagonal Bravais lattice, with the indication of the points of maximal symmetry and (b) the band structure calculated for TiS₂ (from ref. [47])



2.1.3 Synthesis

TMDC single crystals can be prepared by chemical vapor transport [54]. A microcrystalline powder of the compound is filled together with a halogen as transport medium into an evacuated quartz ampoule and placed under a temperature gradient for several days. The gradient is chosen so that the stable phase is the gaseous metal halogenide on the warmer side, and the solid TMDC on the other [55]. The crystal used in this work were provided by Dr Y. Tomm (HMI-Berlin), and prepared under the conditions summarized in Tab. 2.2. For the TaX₂ compounds the thermodynamically stable phase is 2H at RT, while at the synthesis temperature 1T is the stable one. To obtain the 1T phase the crystal is abruptly quenched to RT, while for the 2H phase the temperature is lowered at a 10°C/h rate. During the phase transition the crystal is affected by severe strain, and a large density of cracks and defects results.

High chalcogen pressures must be maintained to obtain the 1:2 metal-chalcogen ratio. Excess metal is incorporated into the octahedral empty sites of the van der Waals gap, affecting the physical properties of the material. Even for stoichiometric crystals Frenkel type disorder is

possible, when a M atom occupies a position in the van der Waals gap instead of in the M plane [56].

crystal	transport agent	temperature gradient	duration
1T-TaS ₂	iodine	920-970°C	10 days
1T-TaSe ₂	iodine	900-950°C	10 days
2H-TaS ₂	iodine	750-870°C	8 days
2H-TaS ₂	iodine	750-870°C	8 days
2H-WSe ₂	selenium	1000-980°C	12 days
1T-TiS ₂	iodine	1000-920°C	10 days
1T-TiSe ₂	selenium	900-800°C	5 days

Tab. 2.2 Preparation conditions for the TMDC single crystals used for this work

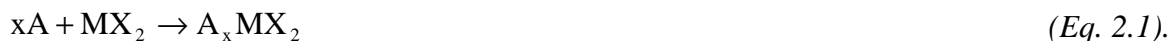
2.2 The intercalation reaction

In this section the concept of intercalation will be introduced with particular emphasis to its relation with TMDCs. Popular reviews on the intercalation in TMDCs are given in references [30-32, 35, 36, 57, 58].

2.2.1 Definition and effects

Some crystal structures contain spaces free of any atom or electronic density of a size, which is comparable, or can be expanded, to that of atoms, ions or (macro-)molecules. Depending on the dimensionality of these regions the resulting lattice can contain cavities, tunnels, planes, or a three-dimensional network that partially or totally may be occupied by guest species. The related insertion phases are called intercalated compounds. Depending on the nature and amount of guest species the intercalated compound may strongly differ in chemical and physical properties from the host compound.

Intercalation compounds can be prepared by direct synthesis [59]. However, if access pathways to the intercalating sites are available, they can also be obtained from the host and guest compounds in an intercalation reaction. If x mol A are intercalated in 1 mol MX₂ the reaction can be written as



Structural effects

In the ideal case the intercalation reaction is considered to be topotactic, which means that the host structure undergoes no distortion. Layered materials are close to the ideal situation because, due to the weak inter-layer interactions, the main effect to the structure is the expansion along the **c** axis with nearly no change within the slab structure. Therefore, beside graphite, TMDCs intercalation compounds are probably the best studied, with a wide range of guests including alkali metals, transition metals [60, 61], non-metals [62], molecules [63] and even polymers [64, 65].

With organic molecules c expansions up to 20 times have been reported [63]. With Li the c expansion is $<0.5 \text{ \AA}$, with Na about 1.5 \AA .

The great adaptability of the host structure has an effect also on the diffusion of the guest, which favors the reaction kinetic. The guest in the van der Waals gap is surrounded by chalcogen atoms. Tetrahedral, octahedral, and trigonal prismatic sites are available, but the occupancy of tetrahedral sites is known only for rare cases (e.g. $\text{Ag}_{0.25}\text{Cr}_{1.09}\text{S}_2$ [56], or $\text{H}_{0.33}\text{TaS}_2$ for 1T-TaS₂ [31]). The octahedral coordination is preferred for Li, while K, Rb, Cs are mainly found in the trigonal prismatic coordination. The occupation of a trigonal prismatic coordination of the guest species requires a sliding of the layers to each other by $a/\sqrt{3}$ along the $(11\bar{2}0)$ direction from the usual close packed structure. This implies for 1T polytypes the transition to the 3R phase. But also with octahedral coordination the slabs may slide into a 3R coordination [30]. Tab. 2.3 reports some possible rearrangements; several other are possible, including alternation of octahedral and trigonal prismatic coordinated layers. For each specific guest/host system different stackings may be observed in dependence of the guest concentration. Rouxel and co-workers carried out the most extensive study on alkali intercalates of group IVb TMDCs [34]. They found that Li shows a single phase over the whole composition range, whereas the other alkali metals form several different phases. Although the trigonal prismatic phase is stabilized by a larger cation, the octahedral coordination may be more stable at higher alkali concentration (Fig. 2.6).

host	intercalated compound	name	guest coordination	<i>Tab. 2.3 Some stacking sequences of intercalated TMDCs, according to ref. [56]</i>
AbC	AbC[c]BcA[a]CaB[b]		Tetrahedral	
AbC	AbC[b]	1T	trigonal antiprismatic	
AbC	AbC[b]CaB[a]BcA[c]	3R(I)	trigonal prismatic	
AbC	AbC[a]CbA[c]	2H(I)	trigonal prismatic	
AbC	AbC[a]BcA[b]CaB[c]	3R(II)	trigonal antiprismatic	

If the expansion induced by intercalation is large, the phenomenon of staging may occur for small guest concentrations. In this case the guest is inserted solely in specific, equidistant van der Waals gaps among all those available, avoiding to loose the favorable layer-layer interaction. Li does not produce appreciable expansion, and in this case no staging phenomenon is observed [66].

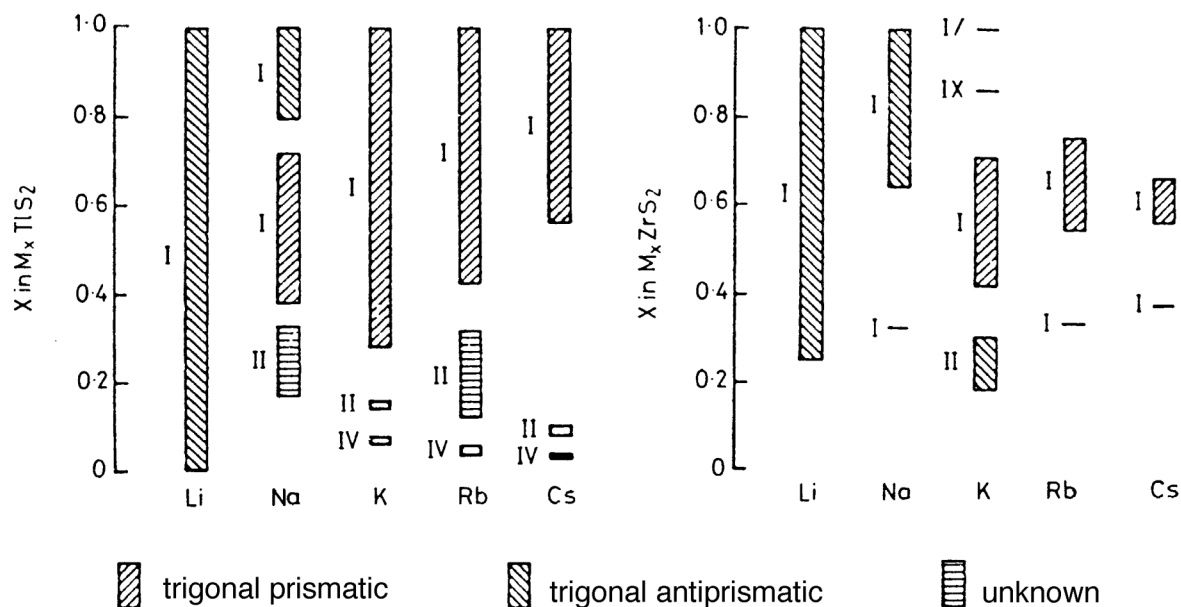


Fig. 2.6 Phases formed by different alkali in TiS_2 and ZrS_2 , after Rouxel [34]

Electronic effects

A redox reaction can accompany the intercalation, if the intercalated species and the host have different electrochemical potential. Electron donors or acceptors can be inserted in graphite. In TMDCs only donor intercalation is known as is the case for alkali intercalation. In this case the intercalation reaction can be written as



The intercalation compound's stability depends dramatically whether the acceptor level is bonding, antibonding or non-bonding. In any case, intercalation always implies changes in bond angles and distances, which are reflected in the electronic structure. But also stabilization of injected electrons can succeed via structural distortions, like Jahn-Teller effects, CDW changes, or even change of transition metal coordination. Li intercalation induces a phase transition $1T \rightarrow 2H$ in TaS_2 [67] and $2H \rightarrow 1T$ in MoS_2 [68]. In the ideal case where such changes can be neglected, the model known as rigid band model (RBM) applies [31, 69]. This model was originally proposed to explain variations of the electronic structure of dilute metallic alloys [70] and a description of different versions is given in ref. [71]. Applied to the alkali intercalation in TMDCs the RBM assumes the total transfer of one electron from the valence s orbital of the alkali guest to partially filled d band of the host. The only observed effect is the progressive filling of conduction band states and the Fermi level moves upwards in the host structure. The rigid band model can be applied, in a first approximation, to systems where electrons are transferred to non-bonding bands, and electron coupling across the intercalated space is weak. The simplification has been considered

satisfactory in a few systems both theoretically (Li/TiS₂ [72, 73]) or experimentally (Li/TiSe₂ [74]). In these cases it was actually found that the alkali valence s electron is transferred to the lowest unoccupied Ti 3d states, without drastic changes of the density of states. However, in general the band dispersion and their relative position can significantly change and must be considered in a more detailed discussion.

In addition to the gain in electronic energy, an ionic term favors the intercalation process, which is due to the electrostatic interaction between the cationic guest and the anionic host lattice. Both electronic and ionic energy gains related to the charge transfer make the redox reaction the driving force for intercalation. This approach of evaluating the reaction energy by considering the two distinct electronic and ionic contributions is based on the rigid band model. It was criticized by some authors, due to the strong ion-host interaction in the intercalation compound: the filling of the empty states would be compensated by the lowering of the band energy due to the potential generated by the positive ion [75, 76]. Calculations of the total energies of intercalated and deintercalated compound with pseudopotential methods can overcome the question [77].

The extents of charge transfer between intercalated alkali and host has been debated for a long time, and still no complete agreement has been reached. Experimental data and calculations based on Mulliken population numbers indicate a wide range of fractional values. The observation that the c lattice expansion from TiS₂ to LiTiS₂ matches the Li ionic radius, which is the half of that found in metallic Li could be taken as proof of a total charge transfer [30]. NMR investigations confirmed the fully ionized state for Li, but as function of its concentration a slight increase of negative charge around Li could be shown [78]. The magnetic susceptibilities of dichalcogenides intercalated with different alkali metals were found to be small, paramagnetic and temperature independent, as typical for metals, and confirm the delocalized nature of the electrons in the intercalated compounds [78].

compound	from Li	to M	to X	method	reference
LiTiS ₂	>0.9			Li ⁷ NMR	[79]
2H-LiTaS ₂	0.45	0.07	0.19	LMTO calculation	[80]
LiTiS ₂	0.24	0.09	0.15	Extended Hückel approximation	[81]
LiTiS ₂	0.96	0.23	0.37	Hartree-Fock calculation	[82]
LiTiO ₂	1	0.26	0.22	Pseudopotential LDA calculation	[77]
LiCoO ₂	1	0.28	0.25	Pseudopotential LDA calculation	[77]
LiCoS ₂	1	0.14	0.15	Pseudopotential LDA calculation	[77]
LiCoSe ₂	1	0.08	0.14	Pseudopotential LDA calculation	[77]

Tab. 2.4 Values of the charge transfer between intercalated metal and the host compound MX₂ as estimated by theoretical or experimental methods. Note that two chalcogen per unit cell are present

Also the spatial distribution of the injected charge cannot be accurately described in a simple model. As the host compounds are not purely ionic, charge cannot be just transferred to reduce the transition metal. According to most calculations [43, 46, 82-84] the chalcogen are hybridized with an important contribution (about 20%) to the t_{2g} and an e_g bands as originated by the octahedral crystal field splitting of the transition metal states. Thus partial electron occupancy of the t_{2g} band suggests a reduction of both transition metal and chalcogen. Sulfur K -edge XANES spectra and calculations of the unoccupied partial S 3p valence states of the Li/TiS₂ system reported in refs. [81, 83] confirm this S 3p-Ti 3d hybridization but also indicate its decrease with intercalation.

A decrease of the hybridization was found in calculations of pseudocompounds with no guest but based on crystallographic data for intercalated compounds [83]. The ionicity was attributed to the structural distortions induced by the host, and not to charge transfer. However, the structure relaxes as a consequence of the intercalation process which also includes charge transfer. Thus the increased ionicity should be considered as the cause of the structural modifications and not the effect. Calculations of the electronic structure of bulk and isolated TiS₂ slabs suggest that with increasing interlayer distance the energetic position of the Ti electrons increases and thus the S-Ti bond covalency also increases [40]. The charge transfer to S implies that intercalation enhances the ionic nature of S and also the ionicity of TiS₂. According to Clerc *et al.* [82] the charge density between the S-Ti bond is affected by a loss of 0.75 electrons upon Li intercalation.

A detailed representation of the charge distribution has been presented by Umrigar *et al.* [43] and it was found that for LiTiS₂ the charge although donated to Ti 3d orbitals, spreads mainly between the S and Li planes. More recent pseudopotential LDA calculations for many lithiated layered oxides and chalcogenides suggest a complete charge donation from Li with prevalent localization around both the transition metal and the chalcogen [77]. For earlier transition metals more charge is donated to the metal and less to the chalcogen. With less electronegative (i.e. heavier) chalcogens charge is less localized.

Competitive reactions

Although TMDC intercalation is thermodynamically and kinetically very favorable, reaction with alkali can lead to substrate decomposition [85-87], if the alkali sulfide formation has a more negative free energy:



Reported cases are for the systems Li/WX₂, Na/SnX₂, as well as for the layered chalcogenide Na/InSe. In such cases the alkali s electron is transferred to states with antibonding character. The intercalated compound may still be observed, but only as a metastable form, in particular at low

alkali concentration, since the decomposition reaction requires 4 alkali atoms per formula unit [87]. Cases of decomposition with metallic TMDCs are not known.

2.2.2 Intercalation in alkali-containing solutions

The thermodynamic driving force for the reaction with alkali metals offers many alternative preparative methods for the corresponding intercalation TMDC compounds. Basically three types are known: reaction with reducing alkali-containing solutions, metal deposition, and electrochemical.

Rüdorff published in 1959 the preparation route of many alkali-intercalated TMDCs via the alkali ammonia technique. Powders were immersed in NH_3 solution of alkali metals at -50°C [21]. The powders were found to incorporate solvated alkali ions, and the remaining ammonia molecules could be eliminated under vacuum or by heating. The reaction with n-butyl-lithium in n-hexane has been widely used later due to its simplicity, effectiveness, and absence of solvation molecules.

2.2.3 Intercalation in UHV

Alkali metal adsorption onto metallic surfaces has been well investigated [88, 89]. The low ionization potential of alkali metals induces a charge transfer when adsorbed on more electronegative surfaces. The creation of a strong dipole alters significantly the work function of the substrate. This treatment has important applications in catalysis and electronics. With the same technique, alkali metals or other hosts have been evaporated onto the surface of the host material, and the intercalation reaction has been demonstrated to occur [26, 27]. This method is particularly simple and useful if applied in UHV environment. The TMDC crystal can be cleaved in vacuum and the metal can be directly evaporated onto the adsorbate-free (0001) surface, and then investigated by a number of surface science techniques [26, 27, 90]. The sample can be intercalated with progressively larger alkali amounts, and subsequently analyzed at each step without any contamination with air; for this reason this preparation method has been called “in situ”. The deposition rate can be easily controlled, but for alkali metals an absolute calibration, such as with a quartz microbalance, is usually difficult, because of sticking coefficients below 1. Only estimations related to surface coverage on non-intercalating substrates can be attempted. For this reason, the deposition rate is typically kept constant, and the amount is controlled with the deposition time. Generally the observed intercalated amount is found to rapidly increase with deposition time first, and then to settle at a limiting value dependent on the metal and the crystal substrate, despite further repeated evaporations [26, 37, 91]. This suggests that a metastable state forms, in which the guest at least initially accumulates in the topmost layers due to a kinetic barrier of diffusion into the non-intercalated phase. When the chemical potential of Na increases the activation barrier becomes smaller and diffusion is eventually obtained [37]. The alkali concentration in the topmost layers is

thus limited, and fully intercalated phases with this method have not been reported in the literature, yet.

Some important differences are found between intercalating and other surfaces. On non-intercalating surfaces the work function decreases very rapidly, a rapid change of 1 eV can be induced by a coverage θ of 10%, but further coverage increase produces a depolarization, and a minimum of work function is observed for $\theta=50\%$. At higher coverage the valence electron may be not completely donated, and the formation of a metal phase is observed at low substrate temperature. At room temperature desorption is observed instead. On intercalating substrates, the work function has a smoother decrease and minima are not observed [74, 92]. The electrostatic repulsion prevents a direct interaction among ions, which remain evenly distributed on the surface. The work function of TMDCs is about 1 eV higher than for most metals. This difference influences the electron transfer from the adsorbed alkali metal. In addition on metals also covalent interaction has been found, whereas on saturated TMDC surfaces only purely electrostatic interactions are expected.

2.2.4 Electrochemical intercalation and batteries

Electrochemically it is possible to achieve the best control on the intercalation rate. TMDCs are electronic conductors, and can be used as electrode in an electrochemical cell of the type shown in Fig. 2.7. The electrolyte contains mobile alkali A^+ ions in a solid or in an organic solution. The counter electrode can be a foil of the alkali metal. At open circuit an EMF is measured, which arises from the difference of the Fermi levels in the two electrodes. The intercalation electrode has a considerably lower level (larger negative electrochemical potential) than the alkali metal. If the electrodes are connected through an external circuit of electronic conductors, electrons will flow from the metal to the host, and the cell will discharge. During this process a reduction (cathodic reaction) occurs at the intercalating electrode and an oxidation (anodic reaction) at the counter-electrode. Hence the first is the cathode and the latter is the anode. Although the electrochemical role of the electrodes is reverted during the opposite process of charging, as a convention in reversible batteries the positive electrode is always indicated as the cathode, and the negative as the anode.

During the cell discharge the flow of negative charge into the cathode is compensated by a migration of positive alkali ions from the electrolyte into the host structure, according to the reaction:



At the anode the removal of electrons is compensated by a release of cations to the electrolyte:



The sum of the two electrochemical half-reactions is the intercalation reaction. As long as the reaction is reversible, the cell can be recharged with the opposite reaction.

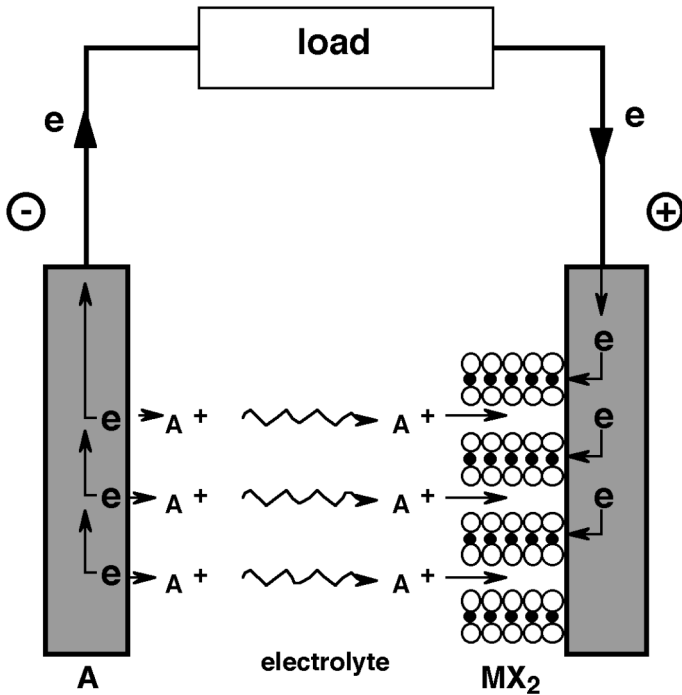


Fig. 2.7 Schematic representation of a rechargeable alkaline cell with a metal at the negative electrode

Origin of the cell potential

The work the electrochemical cell does to transfer an electron from the anode (a) to the cathode (c) through a voltage V is $-eV$. This energy must be equal to the free energy of the corresponding total chemical reaction, that is the transfer of an alkali atom M from the anode to the cathode. The chemical potential μ of a species in a phase is defined as the measure of the free energy variation of the system when a unit of the species is inserted into that phase:

$$\mu = \left(\frac{\partial G}{\partial N} \right)_{p,T} \quad (\text{Eq. 2.6}),$$

with G the free energy variation when N units are inserted. Thus, the electric work equals the difference of alkali metal chemical potential between the two electrodes:

$$-eV = {}_c\mu_A - {}_a\mu_A \quad (\text{Eq. 2.7}).$$

Indeed, the free energy of intercalation can be measured to high precision with the potential of electrochemical cells [75]. If the discharge is done under quasi-equilibrium conditions measurements of $V(x)$ determine the variation of ${}_c\mu_A$, provided the anode has the constant composition of pure A . Eq. 2.7 gives directly the thermodynamic origin of the battery voltage, but a

more detailed insight into different contributions of the driving force for the intercalation reaction has been discussed by Gerischer *et al.* [93], and is summarized hereafter.

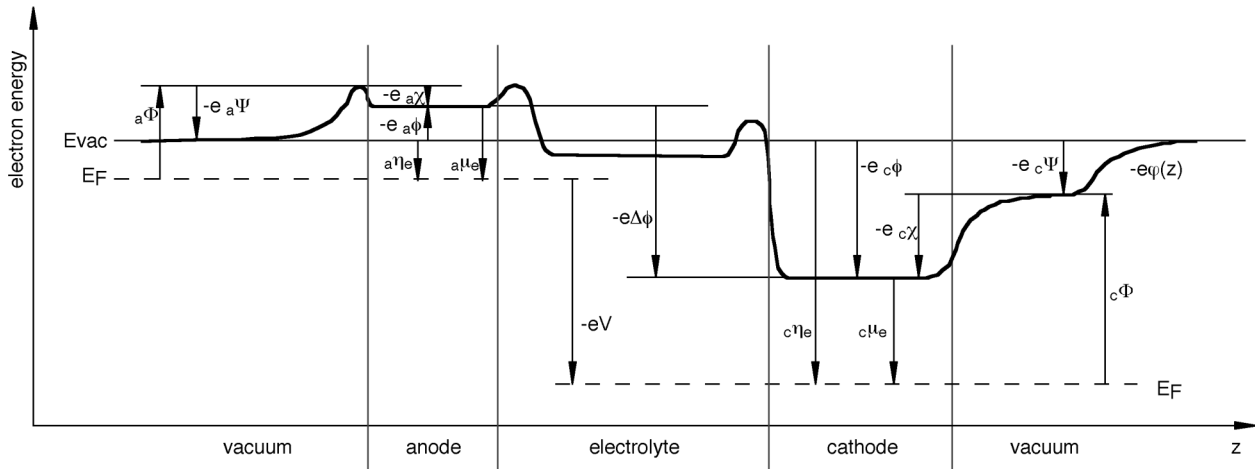


Fig. 2.8 Diagram of the energetic levels in an intercalation electrochemical cell. Given two levels E_1 and E_2 , the arrows point from E_1 to E_2 and their length is $E_2 - E_1$. The profile of the electrostatic potential $\phi(z)$ is only tentative

The electrochemical cell described in Fig. 2.7 can be seen as a system composed by three phases, two electronic conductors separated by an electronic insulator and ionic conductor. The ions A^+ can be exchanged at the interfaces and their electrochemical potential η_{A^+} is the same in the three phases. The cell voltage corresponds to the difference of the Fermi level between cathode and anode. The Fermi level, typically used in solid state physics corresponds to the electrochemical potential of the electrons in electrochemistry. As a definition the electrochemical potential of the species i is a function of the chemical potential μ_i , its charge z_i and the electrostatic potential ϕ inside the phase, which corresponds to the Galvani (or inner) potential ϕ :

$$\eta_i = \mu_i + ze\phi \quad (\text{Eq. 2.8}).$$

The electronic energy difference is given by the difference of electrochemical potential:

$$-eV = {}_c\eta_{e^-} - {}_a\eta_{e^-} = {}_c\mu_{e^-} - {}_a\mu_{e^-} - e({}_c\phi - {}_a\phi) \quad (\text{Eq. 2.9}).$$

At open circuit the cation will attempt to diffuse into the cathode charging it and increasing its Volta potential. This will rise the Galvani potential (which means lowering the corresponding electrostatic potential energy level in the diagram of Fig. 2.8). At equilibrium the electrochemical potential of the ions is the same in the three phases, thus:

$$-e({}_c\phi - {}_a\phi) = {}_c\mu_{A^+} - {}_a\mu_{A^+} \quad (\text{Eq. 2.10}).$$

This expression means that the level of the inner potential in the intercalating electrode is determined by the chemical affinity of the alkali ion in the host lattice, relative to the affinity it has for its pure metallic phase. As a consequence the energetic levels in the cathode assume a well-

defined position with respect to the anode. If we apply this expression for the inner potential to Eq. 2.9 we obtain

$$-eV = ({}_c\mu_{e^-} - {}_a\mu_{e^-}) + ({}_c\mu_{A^+} - {}_a\mu_{A^+}) \quad (\text{Eq. 2.11})$$

or, rearranging

$$V = -(\Delta\mu_{e^-} + \Delta\mu_{A^+})/e \quad (\text{Eq. 2.12}),$$

which means that the EMF of the cell, and therefore the driving force of intercalation can be expressed as function of the two distinct contributions, electronic and ionic chemical potential.

The anode does not change composition, then its chemical potential is constant. Applying to the ions the general relation for the chemical potential, we have

$${}_c\mu_{A^+} = {}_c\mu_{A^+}^0 + kT \ln \frac{{}_c a_{A^+}}{{}_c a_{A^+}^0} \quad (\text{Eq. 2.13}),$$

with ${}_c\mu_{A^+}^0$ and ${}_c a_{A^+}^0$ the potential and the activity of an arbitrary standard state. Therefore an evaluation of the ionic contribution requires the knowledge of the alkali activity coefficient in the host. This must take into account the interactions among the intercalated ions themselves and with the host. Some theoretical evaluations of the chemical potential of the intercalant that take the chemical potential of the ions into account have been attempted [94-98]. They are generally based on lattice-gas models that consider interactions between intercalated species[‡]. An experimental approach for the chemical potential of the electrons in alkali zeolites has been reported by Devautour *et al.* [99, 100] using thermally stimulated depolarization current spectroscopy. This technique can be only applied in electronic insulating materials. In the course of intercalation changes of the local environment of the ions may be thought to be quite smooth. The chemical potential of the ions can then be considered nearly constant compared to the chemical potential of the electrons if at a particular guest concentration the DOS above the Fermi level is small. Based on this assumption several authors could successfully explain the voltage-composition profile of

[‡] In the simplest case these models the Hamiltonian H includes the energy of the interactions of a guest with the host (E_0 , also called site energy) and with other guests (U_{ij}) in the form:

$$H = \sum_i E_0 x_i + \frac{1}{2} \sum_{i,j} U_{ij} x_i x_j$$

where $x_i=1$ or 0, depending whether the site is occupied or not. In general these models split the contributions to the chemical potential in a different manner as assumed in the main text here. The term E_0 considers the electronic and part of the ionic (that responsible of the host interactions with the isolated ionic guest) chemical potential, while the term U_{ij} may consider also interactions of other nature than ionic. The latter term can account also for mutual interactions mediated by elastic deformations of the host lattice. For a detailed description of the different lattice gas models see e.g. ref. [75].

intercalation cells in the frame of the rigid band model by considering the electronic valence structure of the host [101-104]. On the other hand, in presence of energetically inequivalent intercalation sites steps may appear that can be associated to the variations of the chemical potential of the ions when the more favorable site is no more available. In the case of hosts presenting a mix of different sites and of different electron acceptor levels it has been possible to distinguish steps corresponding to a transition of the chemical potential either of the ions or of the electrons [104, 105].

In principle an estimation of the chemical potential of the electrons is possible also by measurements of the work function Φ , e.g. by photoelectron spectroscopy. The electronic contribution can be expressed as

$${}_c\mu_{e^-} = {}_c\mu_{e^-}^0 + \Delta E_F(x) \quad (\text{Eq. 2.14}),$$

where $\Delta E_F(x)$ is the alkali concentration-dependent shift of the Fermi level with respect to the level of the Galvani potential. If the surface potential can be considered constant, the variation of the work function is equivalent to $\Delta E_F(x)$. If the battery voltage is also measured, the ionic contribution would be extrapolated, according to

$$\frac{d}{{}_c\mu_{A^+}} = -e \frac{d}{dx} V - \frac{d}{{}_c\mu_{e^-}} = -e \frac{d}{dx} V - \frac{d}{dx} \Phi(x) \quad (\text{Eq. 2.15}).$$

Unfortunately excluding variations in the surface dipole on the work function is experimentally difficult.

The voltage in a graphite electrode has been compared with its density of states above the Fermi level. Assuming the rigid band model to hold $\Delta E_F(x)$ could be evaluated and it could be estimated that at least for x in Li_xC_6 below 0.1 the electronic contribution dominates [93].

Since ionic and electronic chemical potentials in the cathode are expected to increase, the voltage will decrease with intercalation. But the average voltage can theoretically be predicted with a precision of 10-20% [77, 106]. Using Eq. 2.7 we have:

$$\bar{V} = \int_0^1 V(x) dx = -\frac{1}{e} \int_0^1 [{}_c\mu_A(x) - {}_a\mu_A] dx = -\frac{1}{e} [G_{AMX_2} - G_{MX_2} - G_A] = -\frac{\Delta G_{\text{int}}}{e} \quad (\text{Eq. 2.16}).$$

Given

$$\Delta G_{\text{int}} = \Delta E_{\text{int}} + P\Delta V_{\text{int}} - T\Delta S_{\text{int}} \quad (\text{Eq. 2.17}),$$

the Gibbs free energy can be approximated by the internal energy ΔE_{int} at 0 K, which is of the order of 1-4 eV/molecule. This is correct because the term $P\Delta V_{\text{int}}$ is of the order of 10^{-5} eV/molecule [77], and the term $T\Delta S_{\text{int}}$ is in the range of the thermal energy, about 1% of the internal energy [106]. From total energy calculations of the three structures AMX_2 , MX_2 and M it is then possible

to know the average discharge potential of the cell. Using the same method it would also be possible to compute $V(x)$ if the structural ordering of A in A_xMX_2 could be accurately evaluated. An attempt has been reported in ref. [107].

Despite the importance of a precise understanding of the changes in electronic structure of the host induced by intercalation on the related changes in electrochemical potentials of the electrons, there are only very limited systematic studies yet using photoelectron spectroscopy. One reason is evidently due to the fact that no experimental approach for the investigation of electrochemical cells has been realized so far.

Technological aspects

The electrochemical cell described in this section is a device capable of storing electrical energy, and is the most important application of the intercalation reaction. The idea of using lithium for high density rechargeable batteries dates back to the early sixties. In the mid-seventies the development of intercalation chemistry in layered dichalcogenides introduced significant progresses to the realization of devices of practical interest [24]. Intercalation has not to deal with large kinetic barriers of defect nucleation, diffusion and growth associated with most solid state reactions.

The requirement of lightweight and compact sources for portable electricity in consumer electronics, electric vehicles, and implantable medical devices greatly stimulated basic and applied research aimed to the development of batteries.

As a practical device a battery has to meet several design and material criteria. The composition range over which the alkali metal can be reversibly intercalated determines the battery capacity. High alkali diffusivity is important to satisfy the current-density requirements. A large EFM is desirable, as it will lead to a higher energy density. Given the very low reduction potential and density Li is the preferred alkali metal. The Fermi level position of an intercalation electrode depends from the energy of the top of the valence band. For a sulfide this corresponds roughly to the S 3p level, which is considerably at higher energies than the O 2p level. This difference between a sulfide and an oxide is about 2 V. When in the mid-eighties electrolytes were found, which proved to be stable at high potential, layered oxides $LiMO_2$ have been preferred to the well-established chalcogenides used before. In comparison with sulfides also a higher gravimetric energy density was achieved, given the different atomic mass between O and S.

The design based on a metal anode demonstrated to have serious drawbacks in safety and performance, due to the reactivity of Li and to the difficulty of stripping and plating it on the anode. A much superior performance was achieved with graphite anodes, which are also intercalating electrodes, but at a potential only a few hundred mV higher than metallic Li. This battery design, shown in Fig. 2.9, is called rocking chair or Li-ion, and is particularly useful with layered oxide

cathodes. In fact layered oxides are prepared and are stable only in their intercalated form, while carbons are not. The cell is assembled in the discharged state, and during charging Li^+ migrates from the oxide to the carbon. The cell state depends on which electrode is intercalated.

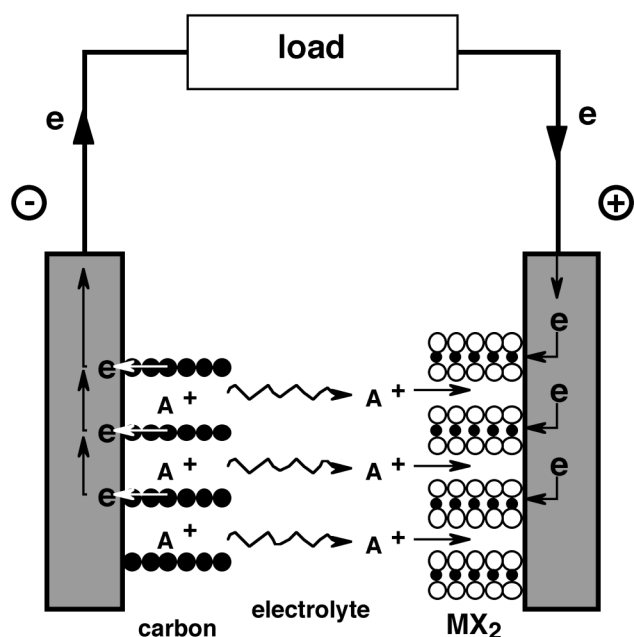


Fig. 2.9 Schematic representation of a rechargeable Li-ion cell

In 1990 Sony introduced the first commercially successful rechargeable lithium battery, a rocking chair cell using LiCoO_2 as positive electrode. With an average potential of 3.6 V it can store more than twice the energy compared with conventional rechargeable batteries of the same size and mass [108-110]. The sale value of this cell already exceeds that of all other rechargeable systems put together, favored by the commercial success of the so-called “3C market”: camera, portable computer, cellular phones.

Present trends in research include the improvement of energy density of the carbon electrodes and the elaboration of cheaper positive electrodes, based on Ni, Mn, Fe oxides, partially substituted by other transition metals. Industrial research concentrates on the improvement of the cell design, of the electrode formulation and of the powder morphology.

Based on the many possibilities offered by solid state chemistry, important improvements can be expected on both performance and fields of application. Thin film deposition technology allows the miniaturization of batteries [111-120]. The monolithical hybridization with non-volatile random access memory or the combination with solar cells will be possible.

Reviews on rechargeable Li batteries are given in refs. [25, 121-129].

2.3 Motivation and outline of the present work

The main goal of this work was to achieve details on the correlation between the electronic structure and the energetics (i.e. the thermodynamics) of intercalation. The position of the Fermi

level, which determines the battery voltage (§2.2.4), depends on the electronic structure. The analytical technique, which can give the most direct picture of the electronic structure is photoelectron spectroscopy. The complete work relied on this tool that will be described in Chapter 3 in reference to this work.

From the electronic structure (i.e. the DOS) the identification of interactions and effects, which are responsible of the mechanism of energy storage is not straightforward. This explains, together with the experimental difficulties to access the electronic structure, why such an uncertainty still exists.

The systematic variation of host and guest nature and concentration is necessary to analyze the effects of the different components on the electronic structure and its modification in the course of intercalation. The approach followed in this work was to experimentally investigate the electronic structure of the intercalation compound as a function of the guest concentration.

The effect of changing the host and the alkali guest has been investigated in §5.1. The aim of this study was to evaluate whether differences could be revealed, which may be easily correlated to the nature of the different atomic species, their sizes and electronic properties.

The most challenging part was to extend the possibilities offered by the typically used technique of UHV alkali deposition on single crystals. In order to achieve a larger range of alkali concentration thin films have been prepared, which solve the problem of the alkali diffusion into the bulk. The preparation and optimization of deposition conditions of thin films are described in Chapter 4. Results of the intercalation on thin films will be reported in §5.2.

The availability of a thin film preparation technique enabled the preparation of an electrochemical cell in which it is in principle possible to simultaneously measure the potential and the chemical potential of the electrons in the intercalation electrode. As assumed in §2.2.4 this will allow the experimental separation of the electronic and ionic contribution to the electrode potential, evidencing the interactions which are able to release most of the energy. The experimental results will be presented in §5.3, while a complete discussion will appear in Chapter 6. The discussion of Chapter 6 will also indicate the possible contribution of photoelectron spectroscopy to the comprehension of the energy storage mechanism in intercalation batteries.